LUND UNIVERSITY

Robotic friction stir welding—Seam-tracking control, force control and process supervision

Karlsson, Martin; Bagge Carlson, Fredrik; Holmstrand, Martin; Robertsson, Anders; De Backer, Jeroen; Quintino, Luisa; Assuncao, Eurico; Johansson, Rolf

Published in:
Industrial Robot

DOI:
10.1108/IR-06-2022-0153

2023

LUND UNIVERSITY

PO Box 117
221 00 Lund
+46 46-222 00 00

Robotic friction stir welding – seam-tracking control, force control and process supervision

Martin Karlsson and Fredrik Bagge Carlson
Department of Automatic Control, Lund University, Lund, Sweden
Martin Holmstrand
Cognibotics AB, Lund, Sweden
Anders Robertsson
Department of Automatic Control, Lund University, Lund, Sweden
Jeroen De Backer
TWI Technology Centre, Sheffield, UK
Luisa Quintino and Eurico Assuncao
University of Lisbon, Lisbon, Portugal, and
Rolf Johansson
Department of Automatic Control, Lund University, Lund, Sweden

Abstract

Purpose – This study aims to enable robotic friction stir welding (FSW) in practice. The use of robots has hitherto been limited, because of the large contact forces necessary for FSW. These forces are detrimental for the position accuracy of the robot. In this context, it is not sufficient to rely on the robot's internal sensors for positioning. This paper describes and evaluates a new method for overcoming this issue.

Design/methodology/approach – A closed-loop robot control system for seam-tracking control and force control, running and recording data in real-time operation, was developed. The complete system was experimentally verified. External position measurements were obtained from a laser seam tracker and deviations from the seam were compensated for, using feedback of the measurements to a position controller.

Findings – The proposed system was shown to be working well in overcoming position error. The system is flexible and reconfigurable for batch and short production runs. The welds were free of defects and had beneficial mechanical properties.

Research limitations/implications – In the experiments, the laser seam tracker was used both for control feedback and for performance evaluation. For evaluation, it would be better to use yet another external sensor for position measurements, providing ground truth.

Practical implications – These results imply that robotic FSW is practically realizable, with the accuracy requirements fulfilled.

Originality/value – The method proposed in this research yields very accurate seam tracking as compared to previous research. This accuracy, in turn, is crucial for the quality of the resulting material.

Keywords Friction stir welding, Robotics, Force control, Seam-tracking control, Control, Sensors, Robot welding

Paper type Research paper

1. Introduction

Friction stir welding (FSW) is becoming an increasingly popular solid-state joining process, known for its superior mechanical properties and its ability to join dissimilar and hard-to-weld materials. FSW was invented in 1991 and patented by The Welding Institute (TWI) (Thomas *et al.*, 1991). General reviews of FSW have been presented by Ma, (2008) and Tanwar and Kumar (2014), and, in particular, a review of robotic FSW has been made by Cook *et al.* (2004). Application of hybrid force/position control was reported by Mendes *et al.* (2014).

In FSW, a rotating, nonconsumable tool is plunged into the interface of the two materials to be welded. The combination of frictional heat and mechanical deformation of the material results in a flow of plasticized material around the tool, which is contained between the tool and the surrounding solid material. This produces a high-quality joint which can reach a tensile

The current issue and full text archive of this journal is available on Emerald Insight at: **https://www.emerald.com/insight/0143-991X.htm**

Industrial Robot: the international journal of robotics research and application
© Emerald Publishing Limited [ISSN 0143-991X]
[DOI 10.1108/IR-06-2022-0153]

The authors acknowledge research funding from the European Commission for the FlexiFab project grant agreement 606156 within the 7th Framework Programme. The LU authors are members of the ELLIIT Excellence Center at Lund University.

Received 3 November 2022
Revised 19 December 2022
2 January 2023
Accepted 8 January 2023

strength exceeding that of the parent material. The materials are not melted and therefore the heat input is low. This implies lower energy consumption and less distortion than in most welding processes. The process allows for high-quality joints, especially in dissimilar joints and hard-to-weld materials, as aluminum alloys. Unlike most welding processes, there is a mechanical interaction between the material and the welding equipment. For FSW, this implies that the actuator operating the welding equipment, e.g. a robot, is subject to high process forces in the order of 1–10 kN for thin plates of aluminum alloys. If a robot is used, this results in deflections of the tool head, which implies that the internal sensors and forward kinematics are not accurate enough for tool positioning (Cook *et al.*, 2004). A standard method to mitigate inaccuracy introduced by deflections is stiffness compliance modeling (Guillo and Dubourg, 2016; Lehmann *et al.*, 2013; Backer and Bolmsjö, 2014). This is based on modeling of joint deflections Δq which can be calculated knowing the torques or the forces, that can both be measured. So, deflections can be determined by equation (1), the later for Cartesian deflections.

$$\Delta q = K_j(\tau) \text{ or } \Delta x = K\big(q, F(q)\big) \quad (1)$$

where τ and F are the joint torques and external forces, respectively, acting on the robot and K a nonlinear compliance function. To avoid the dependence on expensive equipment capable of accurately measuring the deflections, the clamping method has been proposed using arm-side angle measurements, removing the problem of joint deflections (Lehmann *et al.*, 2013; Guillo and Dubourg, 2016). Furthermore, arm-side angle measurements were used by Lehmann *et al.* (2013), removing the problem of joint deflections. However, these methods do not capture deflections if they occur in the links, or in the joints orthogonally to the movement direction, which reduces the resulting accuracy of the model obtained and thus, of the robot. Thus, a robot with deflection compensation must be used for FSW to achieve sufficient accuracy by managing the large machining forces and resulting high deflections. Several developments have been introduced aiming to broaden the range of industrial applications and to improve welded joint properties. Most of these developments have focused on the tool type and configuration, such as stationary shoulder FSW (SSFSW).

This paper presents the work performed to develop a complete robotized system for FSW, measuring the tool position in relation to the weld seam using an external laser sensor seam tracker, closely connected to the tool. Measurements were fed back to the position controller for deflection-compensating action. This approach compensated for the deflections described above. The seam tracking system was experimentally verified when welding thin aluminum joints with a stationary shoulder tool.

1.1 Problem formulation

In this paper, we address the question whether a robot with deflection compensation could be used for FSW with sufficient accuracy, despite the large machining forces, resulting high deflections, and various tool tilt angles. In particular, the FSW tool tip must be within 0.5 mm from the center line of the seam while welding in presence of robot compliance due to machining forces, to guarantee desirable joint quality.

1.2 System requirements

To develop a flexible robotized system for FSW, the main challenges are related to the development of:

- FSW tools suitable for a range of joint configurations operating at relatively low reactive forces, to be compatible with low-cost robotic systems;
- customized welding heads capable of carrying out three-dimensional(3D) welds; and
- closed-loop control system integrating sensors and software to position the robot and the FSW tool to follow the required weld path.

1.3 Previous research

The concept of FSW, using dedicated machines, is explained by Gibson *et al.* (2014). The principles covered include tool design, common defects and material flow. In this present paper, laser was used for perception. Laser has also been used for the welding itself (see, e.g. Kim *et al.*, 2008; Reinhart *et al.*, 2008). Laser was used for perception for grinding by Ge *et al.* (2021). Robotic FSW and the associated challenges due to robot compliance were addressed by De Backer *et al.* (2010). Force measurements were taken, and fed to a compliance model, to estimate path deviations and compensate for these. The model error was in the order of 0.5 mm, and therefore path deviations of that magnitude would be expected after the compensation. Furthermore, previous methods on sensor-based monitoring for FSW are outlined by Mishra *et al.* (2018).

This present paper extends previous research by proposing a new hardware arrangement, based on a laser sensor getting measurements close to the FSW tool, combined with a new hybrid force/motion control law. The main benefit of the proposed approach is the resulting low seam-tracking error. Similar laser sensors have been used for FSW previously, but on dedicated machines as opposed to industrial robots. There are many ways to implement the proposed control law. In this paper, the position control was implemented by the authors in the programming language C, and the force control was realized by ABB IRC5 (ABB Robotics, 2016).

1.4 Motion and force control

In robotic FSW, force control and motion control commonly run in parallel. Such structures are known as hybrid force/motion control or hybrid force/position control (Craig, 1989; Johansson *et al.*, 2014). The control is then decomposed, so that a subspace of the tool's configuration space is force controlled, whereas the complementary space is position controlled. Hence, each dimension of the tool configuration is either force controlled or position controlled.

Which subspaces to force control, and position control, can be determined partly based on natural constraints, which emerge from the interaction between the tool and the environment. The alternatives are limited to:

- position control in directions with natural force constraints;
- force control in directions with natural position constraints.

For instance, the contact force is constrained to be 0 for directions in which free-space movement is possible, and therefore, only position control is supported. Vice versa, if physical contact with the environment prevents movement in a given direction, only force control is possible in that direction.

There might also be directions without natural constraints, and for those the control mode may be determined based on so-called artificial constraints, which in turn are based on the desired behavior of the robot given the task. For instance, the movement could be artificially constrained to follow a reference path. Directions that are artificially constrained imply the opposite control modes, as compared to natural constraints, i.e.:

- force control in directions with artificial force constraints;
- position control in directions with artificial position constraints.

In this paper, we will determine suitable control modes for FSW based on these constraints.

2. Notation

For convenience, Table 1 lists some of the more important quantities used in this work. This notation will be explained in more detail later on, while this list may serve as a quick reference. Further, the coordinate frame used here is shown in Figure 1.

3. Method

In this section, the hardware architecture and software implementation, followed by the control design for seam tracking, are described.

3.1 Hardware architecture

An ABB IRB 7600 robot, displayed in Figures 2 and 3, equipped with a spindle and an interchangeable FSW tool, was used to perform the welding. The spindle was controlled by a programmable logic controller. The work-piece material was attached in a fixture in front of the robot, and a force sensor was mounted between the robot's tool flange and the spindle. Furthermore, an external laser seam tracker manufactured by Meta Systems was attached to the robot (Meta Vision Systems, 2016). It was of great importance to measure the seam position as close to the tool tip as possible, while fulfilling the mechanical constraints that there should be room for the spindle and the seam tracker, and that collision with the fixture should be avoided. To achieve this, a mirror was used to redirect the laser beam, both on its path from the sensor to the work piece, and vice versa. This allowed for measurements 3 cm in front of the tool tip. The design layout is displayed in Figure 1. in (Carlson *et al.*, 2015) showed how to solve the

Table 1 Definition, notation and description of variables

Variable	Description
t	– Sample index
h	– Sample period
$\hat{x}$	– Position measured by seam tracker
x_r	– Reference tool position
Δx	– Change of reference position for EGM
x_e	– Position error
x_i	– Time-integrated position error
K_p	– Proportional gain of outer controller
K_i	– Integral gain of outer controller

Figure 1 Tool coordinate frame $T(x, y, z)\leftrightarrow$ (red, green, blue)

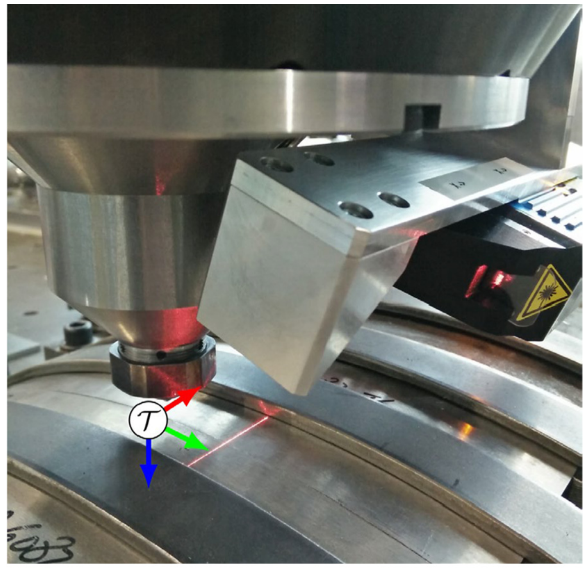

Notes: The z-direction points down perpendicularly to the work-piece material, y is parallel to the seam, and x is perpendicular to the seam and to z. The frame is orthonormal and right oriented

Figure 2 Robot cell used in the experiments

Figure 3 FSW equipment used in the experiments

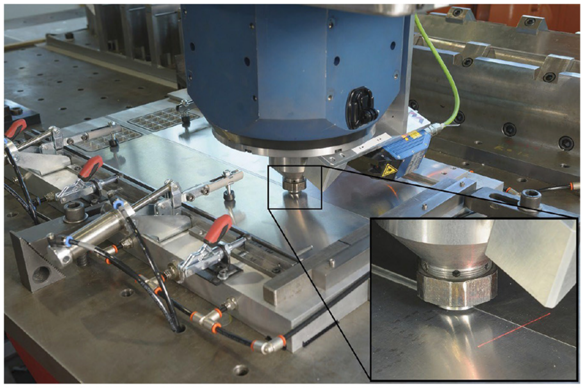

Note: In particular, the stationary-shoulder FSW tool is magnified in the lower-right figure

calibration problem between the sensor and the tool flange of the robot.

One dedicated PC was used to run the controller and sensor communication, and a second PC formed a logging server where process data was stored. This arrangement is elaborated upon in Section 7. The ABB IRC5 system was used to run the low-level robot join controller (ABB Robotics, 2016).

The weld trial runs described herein were based on the SSFSW technique, which is typically used where low heat input and a smooth surface finish are critical.

3.2 Sensors

There are several types of sensors on the market which were assessed for robotized FSW, including tactile, ultrasonic and inductive sensors. Optical sensors are contact free and rely on light reflected from the surface. Laser stripe profilers project one, or several, laser lines onto the surface allowing for a 3D reconstruction of the workpiece surface. They have high resolution (typically 0.05 mm), relatively small field of view and depth of field, and low dependence on surface reflectiveness. Furthermore, they can be mounted sufficiently close to the tool. However, these existing sensors were developed for standard fusion welding processes.

FSW does not exhibit the extreme temperature and lightning conditions of such processes, thus rendering existing sensors unnecessarily expensive and robust. A sensor especially designed for the FSW process would be smaller, cheaper and easier to mount. Vibrations due to the FSW process and not present in standard robotic welding have to be taken into account as well as the integration of the sensor into a real-time system. A sensor with a suitable interface and protocol should be chosen or developed, e.g., using an open protocol. An open protocol that is self-describing, real-time, efficient and replaceable would promote integration without introducing dependencies on that specific protocol. The size and geometry of the sensor determine the placement options of the sensor which, in turn, influence the effectiveness of the sensor. Using a laser sensor gives the possibility to automate the weld seam inspection, either by mounting an additional sensor, or by traversing the same path backward. Laser scanning may be the only sensor type with required precision to inspect the seam. So, an external laser seam tracker from Meta was selected and attached to the robot (Meta Vision Systems, 2016).

A fixturing system was designed with vacuum clamping underneath the sheets, allowing adequate clamping close to the joint line and along the whole weld length. The fixture includes electronically actuated pneumatic valves controlled by the robot.

3.3 Software architecture

The software implemented can be divided into three main parts: RAPID code and controller configuration of the IRC5 robot controller, control algorithm software and system logging software. Previous research on architectures for communication and control in robot cells was conducted by Nilsson and Johansson (1999), Blomdell *et al.* (2005) and Blomdell *et al.* (2010).

The robot controller software must be capable of sending and receiving motion data, as well as receiving RAPID program data. To handle motion data, the ABB Externally Guided Motion (EGM) interface was used. This interface communicated over an Ethernet/UDP socket and sent data encoded in the Google Protobuf format (Google Inc., 2016). When handling RAPID data, the Robot Reference Interface (RRI) was used. The RRI communicated over an Ethernet/UDP connection and sent data in a human-readable XML format. This interface required a description of the server to connect to, and communication with the controller. To handle merging of data arriving at different samples and from different sources, a piece of software called labcommswitch was implemented. The purpose of this software was to allow for generic appending of new data sources and sinks in a type-secure way. The protocol LabComm was used for inter-process communication, as it provided a type-secure way of sending and receiving data among processes (Blomdell, 2016). Logging was separated from the algorithm and sensor software. Even though it was possible to run the logging software on the same PC as labcommswitch, this was not done in the current setup, as motivated in Section. 7. The server received data from Labcomm switch over a websocket connection, as data samples merged to one stream by labcommswitch. Data from running experiments could be graphically depicted in real-time display for a process operator. The web interface could also display data from completed experiments.

During welding, the FSW tool followed a nominal trajectory, approximately along the seam. Force and velocity control were performed in the z- and y- directions, respectively. Position measurements of the tool position in relation to the seam in the x-direction were obtained by the laser seam tracker and used for seam-tracking feedback control. This controller adjusted the position in the x-direction through EGM. Figure 1 depicts the tool coordinate frame, which is orthogonal and right oriented. The z-direction is perpendicular to the material surface, y is parallel to the seam and x is perpendicular to the seam and to z.

In summary, the software developed is a sensor-based seam-tracking system, tailored for joint line detection along multidimensional FSW paths. The software includes a process supervision system which monitors process data online and stores it in a database. The open architecture of the system allows its further expansion with additional sensors and possibilities for online process control.

3.4 Robot control design – force control and seam-tracking control

Hybrid force/position control was applied. First, the subspaces for force control and motion control, respectively, were determined based on natural and artificial constraints; see Section 1.4.

The tool could rotate freely around the x- and y-axes, and therefore the external torques around these axes were naturally constrained to be 0. Further, any rotation of the spindle around the z-axis would be negligible in comparison with the angular velocity of the tool itself, and would therefore not affect the external torque significantly. The full 3D orientation of the tool was therefore position controlled.

A natural position constraint prevented the movement of the tool in the z-direction, and therefore, this direction was force controlled. The reference interaction force was 4 kN. The x-direction was artificially position constrained, because the task required that the tool followed the seam, and therefore position control was applied along x. The control mode in the y-direction could be chosen freely, and in this research, a constant reference velocity was followed. It would also be possible to track a reference contact force, because a sufficiently large force would move the tool through the material along the seam, though we did not do so in this paper.

Before welding, a nominal trajectory along the seam had to be defined. To initiate welding, a search motion was performed by the robot, that moved the tool toward the work-piece at the beginning of the seam. This motion was monitored by the robot's internal sensors only. Once the contact was established, the FSW was performed. Force-sensor feedback was used for force control in the z-direction, while velocity control was used in the y-direction. In this phase, significant error in the position determined by the forward kinematics of the robot was expected, as large contact forces and torques acted on the tool. Therefore, feedback from the laser seam tracker was used to adjust the movement of the tool in the x-direction, possibly yielding small deviations from the nominal trajectory.

For each time step, the seam tracker measurements indicated the position of the tool in relation to the seam in the x-direction. This measured relative position at time step t is denoted $\hat{x}^t$. Further, the reference is denoted $x^t{}_r$. A proportional-integral (PI) controller was used to determine a position reference change Δx^t to send to EGM. The controller determined the error $x^t{}_e$, and then the output Δx^t, according to

$$x^t{}_e = x^t{}_r - \hat{x}^t \quad (2)$$

$$\Delta x^t = K_p x^t{}_e + x_i{}^t \quad (3)$$

where K_p is the proportional gain, and x_i is the integrated error which apart from the anti-windup functionality is updated as

$$x^{t+1}{}_i = x^t{}_i + K_i x^t{}_e h \quad (4)$$

where h is the sample period and K_i is the integral gain. In turn, EGM sent reference values to the low-level robot joint controller. The position regulator hence took the form of a cascade controller, with the EGM system as inner controller and the PI controller described above as the outer. This is illustrated in the block diagram in Figure 4.

4. Experimental validation

It was required to relate the measurements of the laser scanner to the robot coordinate system. The kinematic calibration was performed by using a linear method developed (Carlson *et al.*, 2015). Measurement data were acquired from a set of nonparallel planes where the plane equations and desired rigid transformation matrices were found in a two-step iterative process.

The complete system was experimentally tested in Al alloys. Figure 5 summarizes the materials and joint configurations tested. The tool was based on the SSFSW technique. It was positioned with a 1° tilt angle toward the trailing edge of the tool, to provide additional forging force onto the plasticized material.

The welds were inspected to identify defects, and specimens were removed for microstructural analysis and mechanical tests.

5. Results

The seam tracking system was verified for SSFSW of 2-mm thick AA6082-T6 plates with a step change along the weld path of 1.5 mm. This was within the allowed range of 2 mm path offset to either side of the previous position. As observed in Figure 6, the controller corrected the weld path. Slight surface irregularities can be seen as the correction comes into force, but no weld defects were observed.

The results indicate that the required accuracy was achieved. Figure 7 shows data from following a straight seam. The tool position followed the reference line very closely. The controller kept the measured signal within the required accuracy of 0.5 mm.

5.1 Stationary shoulder friction stir welding of 3-mm thick AA6082-T6 butt joints

Welds were made at a rotation speed of 2,000 rpm and a welding speed of 1,120 mm/min. A very good weld aspect was observed with good alignment. Bending tests to 180° were successful.

Figure 9 depicts a macrograph of a transverse section showing a fully consolidated weld without defects with a good

Figure 4 Block diagram of the position controlled process

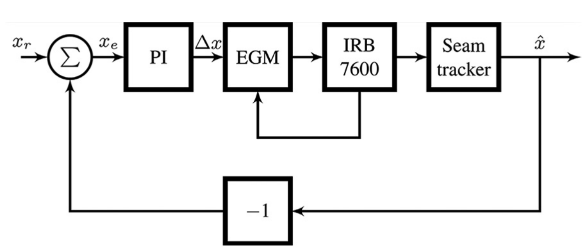

Note: The seam tracker and PI controller formed an outer-control loop. An inner loop was formed by the EGM interface and the IRB 7600 robot system

Figure 5 Materials and joint configurations experimentally tested

Configuration	Aluminium alloy	Thickness (mm)	Geometry
1D	6082-T6 6082-T6	1 3	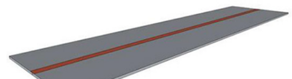
1D Lap	2024 7075-T6	2+2 2+2	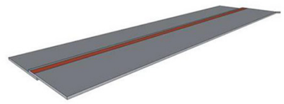
2D Lap	6082-T6	2+0.5	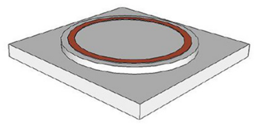
3D Butt	5083	2	
2D Combination	LM25 Body 6082-T6 Lid	1 3	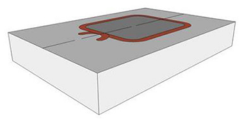
Circumferential butt	6082-T6	4	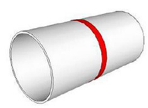

Figure 6 Seam tracking during SSFSW of a 2-mm thick AA6082-T6 butt joint with 1.5 mm step change

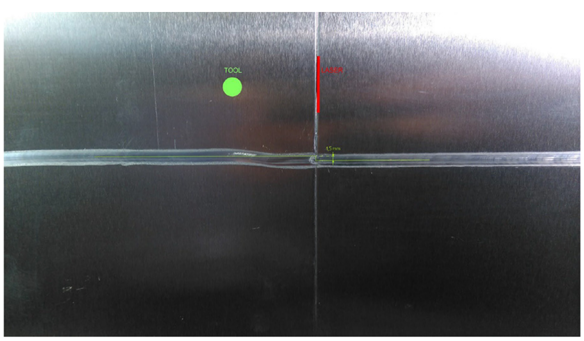

profile. Tensile tests were performed across the welds and one sample failed at 273 MPa on the advancing side. This is approximately 90% of the ultimate tensile strength of the base material and is higher than the minimum value specified in ISO 25239, which is 60%.

5.2 Stationary shoulder friction stir welding of 2-mm thick AA7075-T6 lap joints

AA7075-T6 in lap joint configuration were successfully joined by SSFSW with welding process variables shown in Table 2.

Figure 7 Seam tracker measurements while welding the straight seam

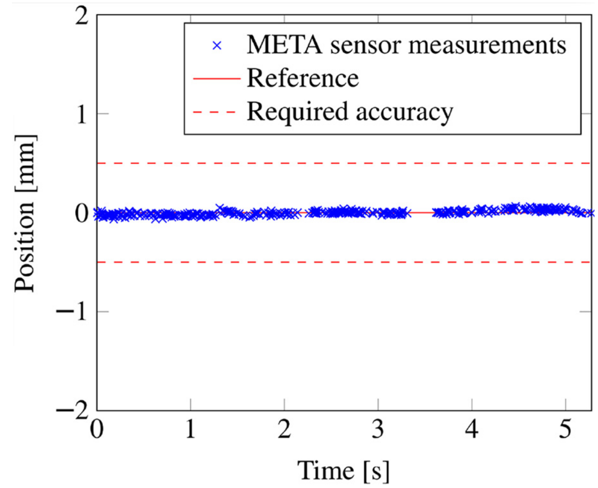

Notes: The controller kept the measured signal within the required accuracy of 0.5 mm. Some severe outliers occurred. These were removed automatically before the controller acted on them, and are not shown here

Figure 8 Seam tracker measurements while welding the straight seam, with an initial step response

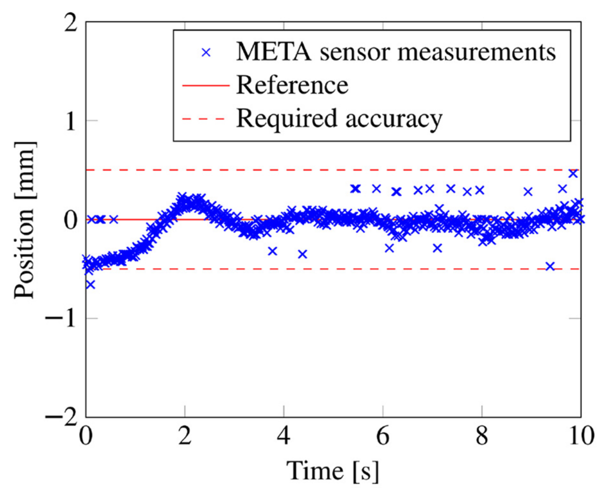

Notes: The controller kept the measured signal within the required accuracy of 0.5 mm. Again, severe outliers occurred. These were removed automatically before the controller acted on them, and are not shown here. However, what seems to be less severe outliers can be seen

Figure 10 shows a macrograph. No volumetric defects could be observed and undercut was smaller than 0.1 mm. Inspection of the joint under higher magnification indicated that a hook, typically observed in lap joints, was present but the height was below 0.1 mm. Results of the bending tests (Figure 11) and the macrographs suggest that when the hook is directed away from the side-under-tension, significantly stronger joints can be obtained.

Figure 9 Macrograph of the weld showing full penetration

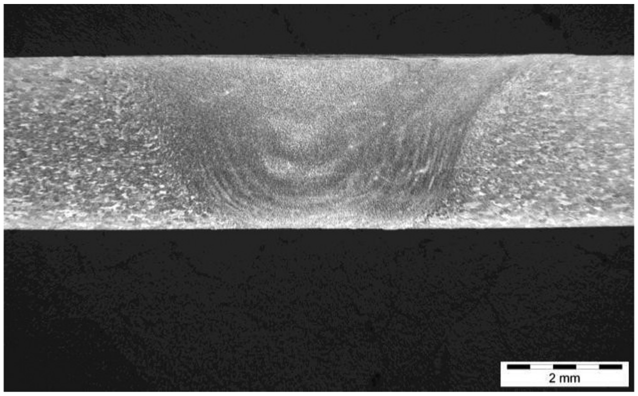

5.3 Stationary shoulder friction stir welding of two-dimensional combination joint

Combination joints refer to configurations such as lid-in-box type applications, where the joint line transfers from a butt joint at the top to a lap joint in the bottom. For this setup, no custom fixture is usually necessary. The box was clamped down to a table and the lid was inserted without clamping. Movement of the lid is geometrically restricted by the box and the SSFSW technique allowed both parts to be welded without the need for additional clamping of the lid. Initially bead-on-plate welds were made to develop the required tool path and obtain welding process variables to produce sound welds.

The FSW variables tested were rotation speed of 2,000 rpm, axial force of 6 kN and welding speed of 10 mm/s. Initial welds showed voids but this could be eliminated by tilting the tool 1° toward the trailing edge of the tool, producing fully consolidated weld sections.

Little evidence of interface hooking could be observed. This has a positive effect on the strength of the weld. However, clear joint line remnants from the vertical interface between the lid and box can be observed. This was expected as the lap welding tool used in the trials promotes mixing in the horizontal plane rather than vertically as with a FSW tool for butt welding.

Figure 11 Successful hammer-S bend test result

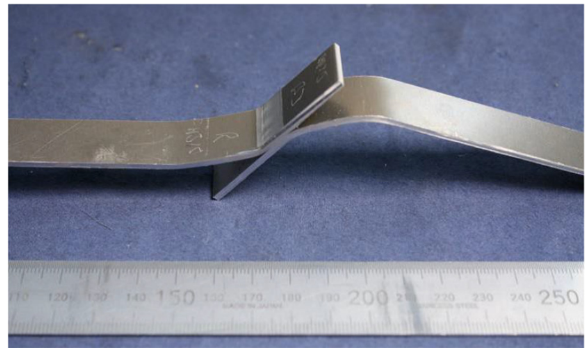

6. Error analysis

Table 3 shows the average absolute value of the control error, for the data shown in Figures 7 and 8, as measured by the laser sensors. In addition to the measured control error, some measurement error is expected. Minor outliers can be seen in the data (Figure 8). Further, the geometric transformation between the sensor and the tool is prone to error. An unobserved rotation of the robot's tool flange around the z-axis, would cause the laser beam to deviate in relation to the tool. For instance, in the presented experiments, the distance between the tool and the laser beam was 30 mm, and a

Table 3 Average absolute value of the control error for the data shown in Figures 7 and 8

Experiment	Mean error (mm)	Variance of error (mm^2)
Constant reference	0.019	0.00059
Step response, after transient	0.069	0.0099

Table 2 Welding process variables for 2 mm thick AA7075-T6 in lap joint configuration

Axial force [kN]	Tool penetration depth (mm)	Rotational speed (rpm)	Welding speed (mm/s)	Ramp distance (mm)	Tilt angle (°)
9	2.0	1000	4	25	1

Figure 10 Macrograph of a AA7075-T6 lap joint with magnification of the interface on retreating (left) and advancing (right) sides

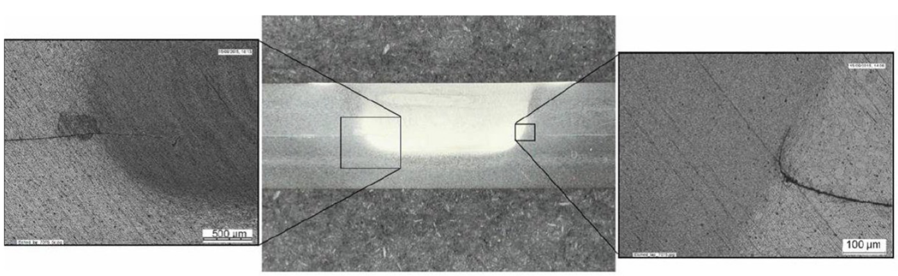

hypothetical rotation of 0.1 degrees would cause a deviation of 0.05 mm. The current setup therefore has room for improvement, and an additional laser beam could be used to observe these types of deviations [see Figure 8 in (Carlson *et al.*, 2016)]. Additional sensors would motivate state-estimation techniques that supports multimodal probability distributions, such as the method based on particle filtering used by Carlson *et al.* (2016) and Carlson (2019).

7. Discussion

The results implied that the required accuracy was achieved. In Figure 7, the measurements seem to follow the reference very closely. However, there was an interval after 3 s where no position measurements were obtained. A probable cause was that the seam tracker obtained ambiguous measurements from the laser reflections, which, in turn, leaves room for improvement. Nevertheless, a visual inspection of the resulting weld showed that the tool had not deviated notably from the seam within this interval.

More transient deviations from the reference appeared in Figure 8. In the transient part, this was because the initial position was purposely erroneous, to excite the controller. There were also more outliers as compared to Figure 7. This was most likely due to small differences in the seams.

The configuration of the mirror must be known for the position estimation. Further, irregularities in the mirror plane would affect the estimation performance. However, no such issue was significant in the experiments performed.

Although many of the implementation aspects presented here would vary for different robot cells, the principles of the position control and laser seam tracker usage would generalize well to other robotic FSW arrangements.

Alternative configurations for implementing custom algorithms were possible. Simpler algorithms could be implemented in a native robotic language such as the ABB RAPID or the KUKA KRL language, as done by Lima and Bracarense (2009). This would suffer the potential drawback of not being powerful enough for computationally demanding algorithms.

Implementing algorithms on a standard PC gave several benefits. More common programming languages such as C, Python and MATLAB could be used, and it facilitated both hardware and software changes.

Dividing the logging and algorithms into two separate parts allowed for easier implementation and reduced code dependence of programs. Another advantage was that errors in logging implementation did not affect the controller software. Maintenance of logging software and server could be done independently of experiments. It also allowed for connection of several robot cells to a single server.

8. Future work

As a next step, trials with a floating-bobbin FSW tool, commonly used for applications where the weld is difficult to support by a backing bar such as hollow extruded profiles, have shown interesting initial results with the method described here. However, a complete and formal evaluation of this usage is left as future work.

In the work presented here, the tool pose was adjusted only in one dimension, perpendicularly to the seam. It remains as future work to make corrections also along the seam, as well as in orientation. In this context, multimodal, non-Gaussian probability distributions of the state based on measurement data are expected. To this purpose, a particle filter algorithm for 6D pose estimation was developed. It was based on input from the robot joint encoders, the laser seam tracker and a 6D force/torque sensor, and was verified in simulations. However, it remains as future work to integrate this state estimation algorithm into the real system, and verify it experimentally.

9. Conclusion

A robotic system was developed for six DOF FSW compensating high deflections due to large contact forces with good accuracy. The system is reconfigurable for batch and short production runs, characteristic of small and medium size company needs.

The system involved the design, manufacturing and testing of dedicated components including hardware, software and monitoring system to have a real-time monitoring and control system. New tools were also developed, such as the reported SSFSW. The presented measurement arrangement with the META laser sensor is new and proved beneficial in the FSW context.

External position measurements were obtained from a laser seam tracker and deviations from the seam were compensated by feedback of the measurements to a position controller. The data logging system captured data from sensors and robot and processed it to provide real-time information on the weld status.

The software developed is a sensor-based seam-tracking system, tailored for joint line detection along multidimensional FSW paths. The software includes a process supervision system that monitors process data online and stores it in a database. The open architecture of the system allows its further expansion with additional sensors and possibilities for online process control.

The robot system was tested on several types of joints with a stationary shoulder tool in different Al alloys, thickness and joint configuration with good results.

The principles described herein generalize well to other robot cells. With the system developed and appropriate FSW tools it was possible to make defect-free welds in 2D and 3D joints and in dissimilar materials and thicknesses in several configurations with improved mechanical properties.

References

ABB Robotics (2016), "ABB IRC5", Accessed: 2022-04-25. ABB Robotics, available at: http://new.abb.com/products/robotics/controllers/irc5 (accessed 25 April 2022).

Backer, J.D. and Bolmsjö, G. (2014), "Deflection model for robotic friction stir welding", In: *Industrial Robot: An International Journal*, Vol. 41 No. 4, pp. 365- 372.

Blomdell, A. (2016), "Labcomm – tools and software", Accessed: 2020-07-22. Dept. Automatic Control, Lund University, available at: https://gitlab.control.lth.se/anders_blomdell/labcomm (accessed 22 July 2020).

Blomdell, A., Dressler, I., Nilsson, K. and Robertsson, A. (2010), "Flexible application development and high-performance motion control based on external sensing and reconfiguration of ABB industrial robot controllers", *Proc. 2010 IEEE Int. Conf. Robotics and Automation (ICRA2010)*. Anchorage, AK, pp. 62-66.

Blomdell, A., Bolmsjö, G., Brogårdh, T., Cederberg, P., Isaksson, M., Johans-son, R., Haage, M., Nilsson, K., Olsson, M., Olsson, T., Robertsson, A. and Wang, J.J. (2005), "Extending an industrial robot controller – implementation and applications of a fast open sensor interface", *IEEE Robotics and Automation Magazine*, Vol. 12 No. 3, pp. 85-94.

Carlson, F.B. (2019), "Machine learning and system identification for estimation in physical systems", Doc. No. TFRT-1122. PhD thesis. Lund, Sweden, Lund University, Dept. Automatic Control.

Carlson, F.B., Johansson, R. and Robertsson, A. (2015), "Six DOF eye- to-hand calibration from 2D measurements using planar constraints". *Proc. 2015 IEEE/RSJ Int. Conf. Intelligent Robots and Systems (IROS2015)*. Hamburg, Germany, pp. 3628-3632.

Carlson, F.B., Karlsson, M., Robertsson, A. and Johansson, R. (2016), "Particle filter framework for 6D seam tracking under large external forces using 2D laser sensors", *IEEE/RSJ International Conference on Intelligent Robots and Systems (IROS)*. Oct 9– 14, Daejon, South Korea, pp. 3728-3734.

Cook, G.E., Crawford, R., Clark, D.E. and Strauss, A.M. (2004), "Robotic friction stir welding", In: *Industrial Robot: An International Journal*, Vol. 31 No. 1, pp. 55-63.

Craig, J.J. (1989), *Introduction to Robotics: Mechanics and Control*, 2nd ed., Prentice Hall, Upper Saddle River, NJ.

De Backer, J., Soron, M., Ilar, T. and Christiansson, A.-K. (2010), "Friction stir welding with robot for light vehicle design", *8th International Friction Stir Welding Symposium, Timmendor- Fer Strand, Germany 18-20 May 2010*, The Welding Institute.

Ge, J., Deng, Z., Li, Z., Li, W., Lv, L. and Liu, T. (2021), "Robot welding seam online grinding system based on laser vision guidance", In: *The International Journal of Advanced Manufacturing Technology*, Vol. 116 No. 5, pp. 1737-1749.

Gibson, B.T., Lammlein, D.H., Prater, T.J., Longhurst, W.R., Cox, C.D., Ballun, M.C., Dharmaraj, K.J., Cook, G.E. and Strauss, A.M. (2014), "Friction stir welding: process, automation, and control", In, *Journal of Manufacturing Processes*, Vol. 16 No. 1, pp. 56-73.

Google Inc (2016), Accessed: 2022-04-26, available at: https://code.google.com/p/protobuf/

Guillo, M. and Dubourg, L. (2016), "Impact and improvement of tool deviation in friction stir welding: weld quality and real-time compensation on an industrial robot", In: *Robotics and Computer-Integrated Manufacturing*, Vol. 39, pp. 22-31.

Johansson, R., Nilsson, K. and Robertsson, A. (2014), "Force control", in Nee, A. (Ed.), *Handbook of Manufacturing Engineering and Technology*, Springer, London, pp. 1933-1965.

Kim, C., Kim, J., Lim, H. and Kim, J. (2008), "Investigation of laser remote welding using disc laser", *Journal of Materials Processing Technology*, Vol. 201 Nos 1/3, pp. 521-525.

Lehmann, C., Olofsson, B., Nilsson, K., Halbauer, M., Haage, M., Robertsson, A., Sörnmo, O. and Berger, U. (2013), "Robot joint modeling and parameter identification using the clamping method", *IFAC Conf. Manufacturing Modelling, Management and Control (MIM2013)*, Saint Petersburg, Russian Federation, pp. 843-848.

Lima, E.J. and Bracarense, A.Q. (2009), "Trajectory generation in robotic shielded metal arc welding during execution time", *Industrial Robot: An International Journal*.

Ma, Z. (2008), "Friction stir processing technology: a review", *Metallurgical and Materials Transactions A*, Vol. 39 No. 3, pp. 642-658.

Mendes, N., Neto, P. and Loureiro, A. (2014), "Robotic friction stir welding aided by hybrid force/motion control", *Proc. 2014 IEEE Emerging Technology and Factory Automation (ETFA) Emerging Technology and Factory Automation (ETFA)*. Barcelona, Spain.

Meta Vision Systems (2016), "Meta vision systems", www.meta-mvs.com/ (accessed April 25 2022).

Mishra, D., Roy, R.D., Dutta, S., Pal, S.K. and Chakravarty, D. (2018), "A review on sensor based monitoring and control of friction stir welding process and a roadmap to industry 4.0", *Journal of Manufacturing Processes*, Vol. 36, pp. 373-397.

Nilsson, K. and Johansson, R. (1999), "Integrated architecture for industrial robot programming and control", *J. Robotics and Autonomous Systems*, Vol. 29 No. 4, pp. 205-226.

Reinhart, G., Munzert, U. and Vogl, W. (2008), "A programming system for robot-based remote-laser-welding with conventional optics", *CIRP annals*, Vol. 57 No. 1, pp. 37-40.

Tanwar, P. and Kumar, V. (2014), "Friction stir welding: review", In: *Int. J. Enhanced Research in Science Technology and Engineering*, pp. 172-176.

Thomas, W.M., Nicholas, E.D., Needham, J.C., Murch, M. G., Temple-Smith, P. and Dawes, C.J. (1991), "Improvements relating to friction stir welding", *US Patent No*, Vol. 5 No. 460, p. 317.

Corresponding author

Martin Karlsson can be contacted at: martin.karlsson@control.lth.se